# High-resolution photoemission study of the electronic structure of the noble-metal (111) surfaces

S. D. Kevan and R. H. Gaylord
*Physics Department and Materials Science Institute, University of Oregon, Eugene, Oregon 97403-1274*
(Received 15 May 1987)

High-resolution angle-resolved photoemission studies of the (111) surfaces of copper, silver, and gold are reported which investigate in detail the properties of the intrinsic surface states located in the projected *sp*-band gaps at the center of the surface Brillouin zones. Accurate two-dimensional energy dispersion relations are reported for each surface state and are quantified in terms of effective masses at the surface Brillouin-zone center. The masses for the three metals are found to be remarkably similar when normalized to the effective mass of the lower edge of the bulk continuum. The decay length of the surface state wave function into the surface was determined for all three surfaces. These results are expressed in terms of an effective mass of the complex dispersion relation within the projected band gap. In accord with our previous results on the copper state, these effective masses are found to be anomalously large by approximately a factor of 2 relative to expectations based on effective mass theory coupled to first-principles bulk band calculations. An explanation of this anomaly involving the nonorthogonality of effective-mass-theory-derived states is explored. All experimental results are compared to the predictions of recent self-consistent surface electronic structure calculations for these surfaces.

## I. INTRODUCTION

The accurate characterization and fundamental understanding of nominally clean surface electronic structure is a subject of significant current interest due to the variety of surface processes which it governs.[1,2] The evolution of precise high-resolution angle-resolved photoemission (ARP) experiments complemented by sophisticated self-consistent codes for surface electronic structure calculations is providing a growing data base from which one can evaluate the current understanding in the field.[3,4] Of central importance in these comparisons is the characterization of intrinsic electronic surface states existing on nominally clean surfaces.

From a global point of view, a surface state can be viewed as a localized eigenstate which is associated with a macroscopic defect; the surface. The ability to prepare clean and ordered surfaces with a high degree of reproducibility allows detailed studies which are not presently possible on other types of defects. For instance, one can easily perturb a surface state in a controlled fashion by adding small quantities of surface contaminants, thereby varying the potential in the dipole layer and adding isolated scattering centers.[5,6] In addition, under optimal circumstances, the decay of the surface state wave function into and its interaction with the bulk can be isolated for study. Finally, the interplay of surface electronic and geometric structures can be probed with a degree of sophistication which cannot be attained for other types of defects.

The purpose of the experiments described here was to characterize as accurately as possible the intrinsic surface states localized in the projected *sp*-band gaps of the noble-metal (111) surfaces using the high-resolution angle-resolved photoemission technique. These states have been observed and characterized by several previous studies.[7–18] However, no high-resolution studies of the silver and gold surface states exist, and precise and reliable experimental data are lacking. Recent self-consistent surface electronic structure calculations of Ag(111) (Ref. 19) and Au(111) (Ref. 20) can be effectively compared to new ARP experiments. In addition, these two surfaces are qualitatively similar to the better-studied Cu(111) surface for which several calculations exist which are in excellent accord with experiment.[21–24] Characterization of the systematic similarities and differences in intrinsic surface state properties such as energy dispersion relation and characteristics of the surface state wave function is thus a useful endeavor.

In particular, recent experiments on Al(111) and Cu(111) have demonstrated the ability of ARP to measure the surface state evanescent decay lengths into the bulk.[16,24,25] The decay length for the Cu(111) surface state was found to be anomalously short relative to the predictions of simple nearly-free-electron and effective-mass theories.[25] Similar studies have also been reported to measure the decay length of the Ag(111) state,[14,18] but have been interpreted to draw significantly different conclusions. This disparity will be examined more closely below. If our results are generalized, they would ultimately affect the predictions of simple theories for a variety of solid-state phenomena, including interband tunneling, metal-insulator transitions, and the sizes of excitonic states. Increasing the number of systems for which such measurements have been performed will help in obtaining a complete understanding of these phenomena. In the present study we have found that the states on Ag(111) and Au(111) have bulk penetration lengths which are also anomalously short, as in copper. A simple explanation is proposed which questions the accuracy of effective-mass theory in predicting these evanescent decay lengths due to the introduction of an overcomplete basis set and the consequent inability to ensure orthogonality between the defect state and the bulk

 ©1987 The American Physical Society

states which are nearby in energy.

Finally, the Au(111) surface is known to reconstruct to form a large unit cell.[26–28] There has been speculation that this reconstruction might be the result of a charge-density-wave instability.[26] Accurate studies of the two-dimensional Fermi surface will shed light on this matter.

The outline of this paper is as follows. Section II discusses the experimental details. Section III presents various experimental ARP results which allow a characterization of the surface electronic structure of these surfaces. Section IV discusses the results and extracts the information outlined earlier, and Sec. V summarizes our conclusions in relation to generalized gap states.

## II. EXPERIMENTAL PROCEDURES

Single-crystal discs were spark cut to within $\pm 0.5^{\circ}$ of the [111] axial orientation and polished by standard metallographic techniques to 0.05 $\mu$m smoothness. Before insertion into the photoemission spectrometer, each crystal was electropolished as described in Tegart.[29] After a few cycles of neon-ion bombardment (10 A/cm$^2$, 0.5 kV, 20 min) and annealing (typically 500 °C, 5 min), excellent low-energy electron diffraction patterns were obtained. For Au(111), at some primary energies, a six-fold splitting of the integral order beams was apparent, indicating the presence of the large-scale reconstruction observed previously.[26–28] Auger electron spectroscopy showed no significant surface contamination, and the crystal surfaces were observed to be stable for long periods of time at the base pressure of typically $1-2\times 10^{-10}$ torr.

Photoemission experiments were performed on the ultraviolet ring at the National Synchrotron Light Source at Brookhaven National Laboratory. The 6-m toroidal grating monochromator and the high-resolution electron spectrometer have been described previously.[30,31] The combined energy resolution was $<60$ meV below 25 eV photon energy and $<100$ meV at higher energies. The angular resolution was typically 1.0°, full width at half maximum.

## III. EXPERIMENTAL RESULTS

### A. Identification of surface states

Experimental results for the Cu(111) surface have been reported earlier,[17,25] so we concentrate here on new data collected from Ag(111) and Au(111). ARP energy distribution curves (EDC's) of the Ag(111) valence band collected at emission normal to the surface are shown in Fig. 1 for 32 eV $\leq h\nu \leq 65$ eV. The $d$-band region, between 4 and 8 eV binding energy, is characterized by several features whose energetic positions can be related to the bulk silver electronic structure. Above and below the $d$ bands, at binding energies of $0.12\pm 0.01$ eV and $7.2\pm 0.1$ eV are two features which resonate in intensity near $h\nu=45$ eV and $h\nu=51$ eV, respectively. The feature near the Fermi energy $E_F$ does not disperse as the photon energy is varied, and has previously been identified in studies at lower photon energies as an intrinsic surface state located in the projected $sp$-band gap along the $\Gamma\rightarrow L$ line of the bulk silver band structure.[8–10,12] This surface state is seen to possess a very narrow energy width. Our observed linewidth of 70–80 meV is significantly less than observed previously due to our improved resolution. Moreover, this width is dominated by the experimental resolution. The natural linewidth is very likely less than 50 meV. This observation calls into question the conclusions concerning the anomalous broadening of this state from inverse photoemission studies reported elsewhere.[32] The resonance in intensity observed in Fig. 1 is similar to that observed on Cu(111) at a photon energy near 70 eV.[16,25] The reasons for the observed shift in photon energy at which the intensity maximizes will be explored shortly. While the state's sensitivity to contamination was not tested due to the inert nature of this surface, there is little doubt that the feature observed near $E_F$ in Fig. 1 is indeed the same intrinsic surface state observed previously at lower photon energy.

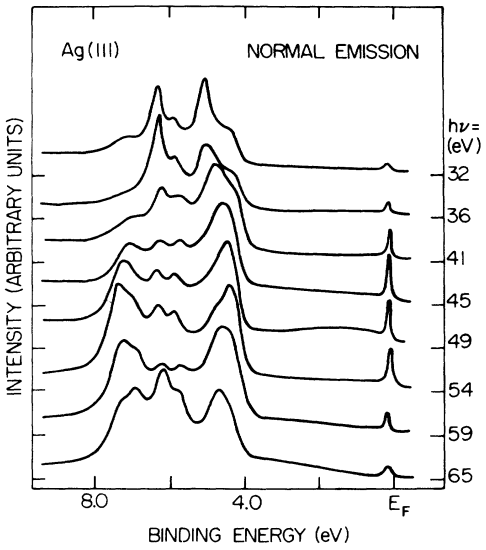


FIG. 1. Angle-resolved photoemission energy distribution curves collected at normal emission from an Ag(111) surface for photon energies between 32 and 65 eV. The light is $p$ polarized at an incidence angle of 60° in the $\Gamma LUX$ plane of the bulk Brillouin zone. The sharp feature near the Fermi level which maximizes in intensity relative to the silver $d$ bands between 4 and 8 eV binding energy at a photon energy near 45 eV is the intrinsic surface state under consideration located in the projected $sp$ band gap at $\bar{\Gamma}$.

The same degree of certainty cannot be maintained for the feature lying below the $d$ bands resonating near $h\nu=51$ eV. Its behavior is qualitatively similar to that observed for a similar feature on Cu(111) labeled $S_3$ in Ref. 14 which was identified as a surface state existing in the $sd$ projected gap along $\Gamma\rightarrow L$. While that assignment was subsequently questioned,[33] it was later shown that the observed state's binding energy is clearly in the gap, and that the intensity cannot arise simply from indirect transitions from band 1 near the $L$ point of the bulk band structure.[17] The energy of band 1 at the $L$ point of the silver band structure has not been measured

by photoemission accurately enough for similar confirmation in this case. A recent calculation of the Ag(111) surface electronic structure does not predict this state.[19] Further experimental and theoretical treatment of the *sd* state will be required to determine whether this state on Ag(111) is an intrinsic surface state or not. For now, we focus our attention on the state above the *d* bands.

The results for Au(111) shown in Fig. 2 for 32 eV $\leq h\nu \leq 67.5$ eV are similar to those shown in Fig. 1 for Ag(111). The high-lying surface state is observed at a binding energy of $0.41 \pm 0.01$ eV, in accord with previous observations.[8,10,13,15] This state on the gold surface is easily observable over a broader range of photon energy than the analogous state on silver, being clearly visible from threshold to $h\nu > 120$ eV and resonating near 43 eV. The low-lying state in gold appears at a binding energy of $7.8 \pm 0.1$ eV. A recent calculation for this surface predicts a well-defined surface state at a binding energy of $\sim 7.0$ eV.[20] As was the case in silver, however, it is at present difficult to ascertain whether or not this state near the *sd* projected band gap is indeed an intrinsic surface state.

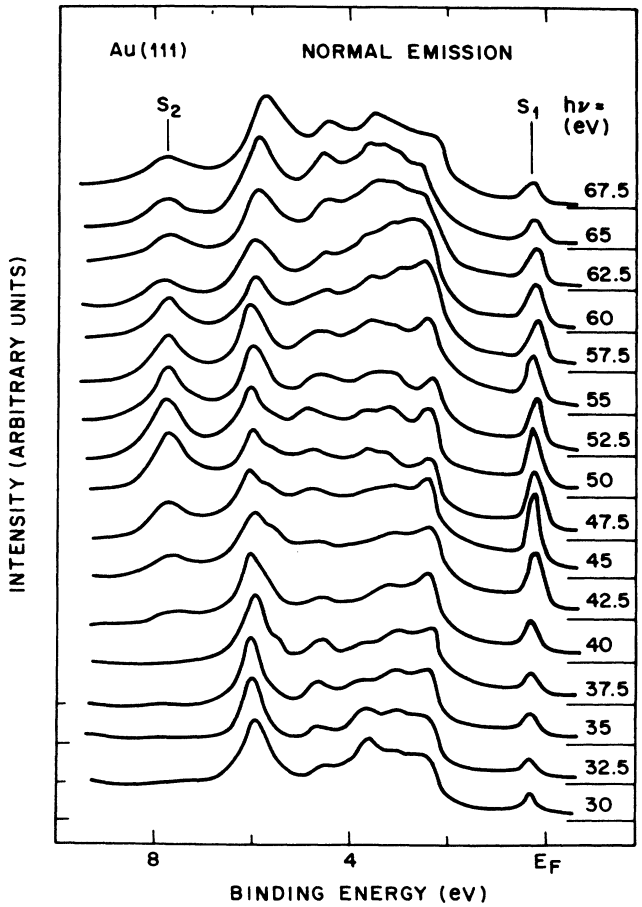


FIG. 2. Angle-resolved photoemission energy distribution curves collected at normal emission from an Au(111) surface for photon energies between 30 and 67.5 eV. The light is *p* polarized at an incidence angle of 60° in the $\Gamma LUX$ plane of the bulk Brillouin zone. The sharp feature near the Fermi level ($E_F$) which maximizes in intensity relative to the gold *d* bands between 2 and 6 eV binding energy at a photon energy near 43 eV is the intrinsic surface state under investigation located in the projected *sp* band gap at $\bar{\Gamma}$.

### B. Dispersion relations

Figures 3 and 4 show expanded EDC's of the high-lying *sp* surface state on Ag(111) and Au(111), respectively, as a function of emission angle measured from the normal. A parabolic dispersion, symmetric about the normal, is evident in each case, in accord with previous results on Cu(111) and Au(111).[7,9–11] The close proximity of the state on Ag(111) to the Fermi level has made an accurate and reliable determination of its energy dispersion relation in the past very difficult. An earlier study, for instance, detected very little dispersion at all.[10] This result was later used to draw conclusions about anomalous broadening of this state due to its close proximity to the bulk continuum.[32] The higher resolution used in collecting the data shown in Fig. 3 shows very clearly the parabolic dispersion and associated Fermi

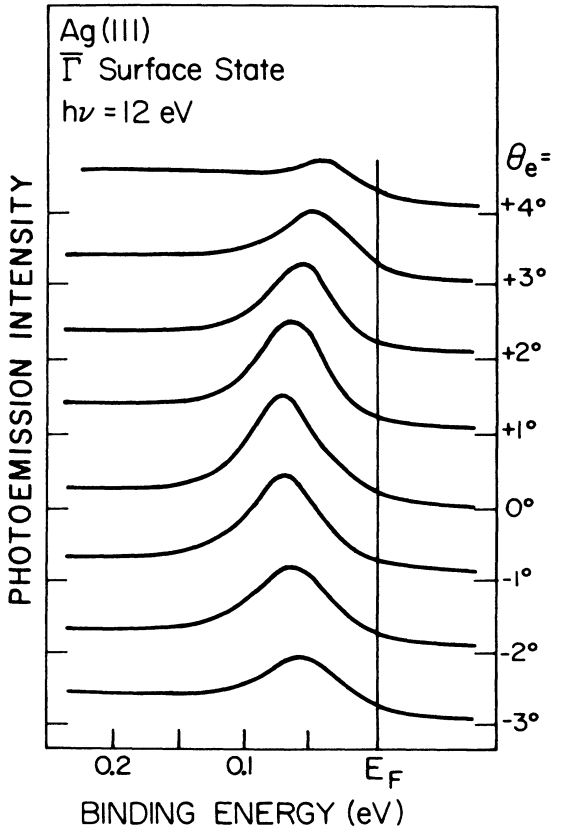


FIG. 3. High-resolution angle-resolved photoemission energy distribution curves of the Ag(111) *sp* surface state as a function of emission angle at a photon energy of 13 eV. The light is *p* polarized at an incidence angle of 60° in the $\Gamma LUX$ plane of the bulk Brillouin zone. Electrons are collected in the same plane. Note the parabolic dispersion about normal emission, shown graphically in Fig. 5.

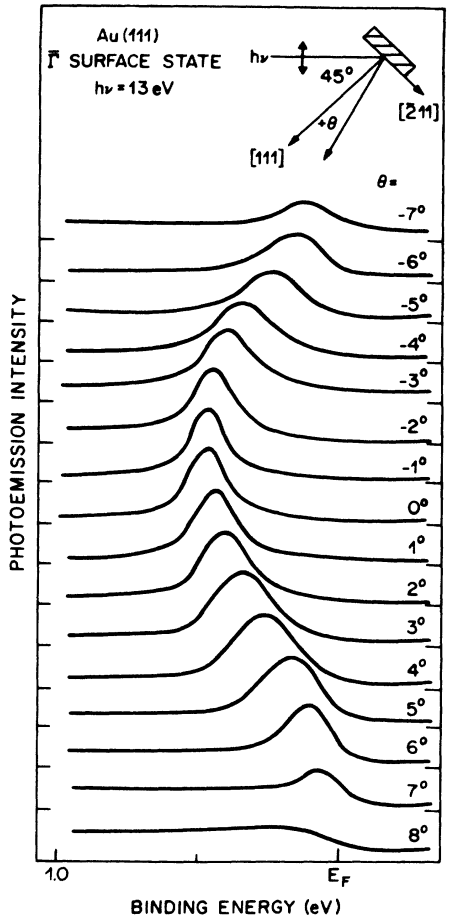


FIG. 4. High-resolution angle-resolved photoemission energy distribution curves of the Au(111) *sp* surface state as a function of emission angle at a photon energy of 13 eV. The light is *p* polarized at an incidence angle of 60° in the $\Gamma LUX$ plane of the bulk Brillouin zone. Electrons are collected in the same plane. Note the parabolic dispersion about normal emission, shown graphically in Fig. 6.

level crossings. The maximum binding energy is greater than our observed energy width, and the band is clearly below $E_F$ at the zone center. Any conclusions about anomalous broadening mechanisms appear to be unfounded.

By converting the emission angles into parallel momenta, a dispersion relation can be determined. The results for silver and gold are shown in Figs. 5 and 6, respectively. The effective mass $m_s$ of these dispersion relations in terms of the free electron mass $m_e$ and the maximum binding energy $E_0$, both measured at the center of the surface Brillouin zone $\bar{\Gamma}$, are determined from a least-squares analysis. These results are shown along with previous results from Cu(111) in the first two rows of Table I. The fitted dispersion relations plotted in Figs. 5 and 6 match the experimental data very well.

The deduction of the bulk continuum, shown shaded in Figs. 5 and 6, is significant in the analysis that follows. The Fermi level crossings of this edge can be obtained quite accurately from the radius of the neck of

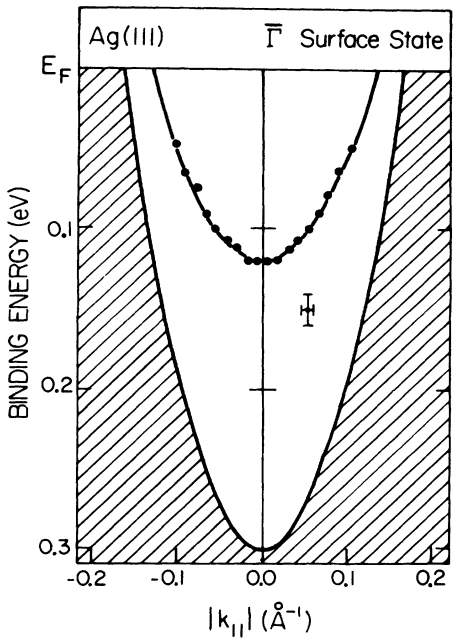


FIG. 5. Energy dispersion relation for the Ag(111) surface state derived from the data shown in Fig. 3. The solid curve is a parabolic fit to our data and yields the effective mass shown in Table I.

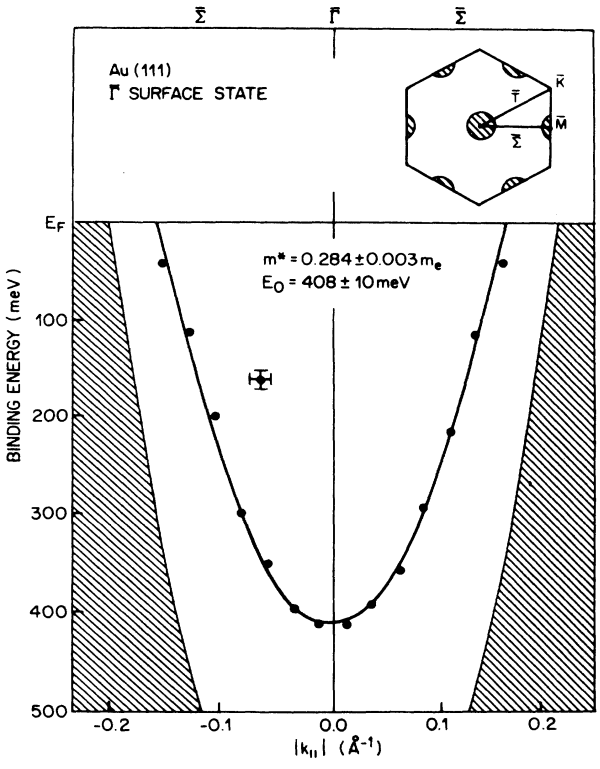


FIG. 6. Energy dispersion relation for the Au(111) surface state derived from the data shown in Fig. 4. The solid curve is a parabolic fit to our data and yields the effective mass shown in Table I.

TABLE I. Summary of results for *sp* surface states on the (111) noble-metal surfaces.

| | Cu(111) | | Ag(111) | | Au(111) | |
|---|---|---|---|---|---|---|
| | Expt. | Calc.[a] | Expt. | Calc.[b] | Expt. | Calc.[c] |
| $E_0$ (eV) | 0.39(1) | 0.58 | 0.12(1) | 0.19 | 0.41(1) | 0.26 |
| $m_s/m_e$ | 0.46(1) | 0.37 | 0.53(1) | 0.24 | 0.28(1) | 0.17 |
| $E_B$ (eV) | 0.82(3) | 1.12 | 0.30(2) | 0.43 | 0.90(3) | 0.96 |
| $m_s/m_B$ | 1.48(2) | 1.2 | 1.56(2) | 1.3 | 1.35(2) | 1.1 |
| $k_F$ (Å$^{-1}$) | 0.217(5) | 0.24 | 0.129(5) | 0.11 | 0.173(5) | 0.11 |
| $\varepsilon_s$ (eV) | 0.41(4) | 0.54 | 0.18(2) | 0.24 | 0.49(4) | 0.70 |
| $m^*/m_e$ | 0.58(8) | | 0.28(6) | | 0.34(6) | |
| $\lambda_s$ (Å) | 4.0(1.0) | 4.5 | 8.7(1.5) | | 5.0(1.0) | |

[a]Reference 18.
[b]Reference 16.
[c]Reference 17.

the bulk Fermi surface, measured to be 0.257, 0.165, and 0.216 Å$^{-1}$ for copper, silver, and gold, respectively.[34] The energy of the edge of the continuum at the center of the surface Brillouin zone corresponds to the $L_6^-$ point of the relativistic bulk band structures. The energies of these points for the noble metals have been difficult to calculate exactly from first principles in the past.[35] We have estimated them using the following method: a combined interpolation scheme[36] was used to calculate the edge of the bulk continuum. $k_F$ was then fixed at the momentum corresponding to the measured Fermi wave vectors, and the value of the $L_6^-$ points relative to the Fermi energy $E_F$ were thus deduced. The rms energy uncertainty of ±0.2 eV in the interpolation calculation is largely canceled by this procedure. Since the curvature of the calculated band is expected to be accurately reproduced, we expect our estimates of the band energies at $L_6^-$ relative to $E_F$ to be very accurate. The energies at the bottom of the continua thus deduced are shown for the three metals in the third row of Table I. These values are in excellent accord with those derived from a variety of optical measurements.[35] The value for Cu(111) can, in addition, be checked with an accurate value determined by ARP measurements, and is within the experimental uncertainty of ±0.03 eV.[17,25] The value derived for Ag(111) is predicted to be accurate to within ±0.02 eV since the extrapolation from the Fermi surface data in that case is very small. In the previous studies which attempted to determine the decay length of the surface state on Ag(111),[14,18] a much smaller value of the energy splitting was derived. Both this splitting and the measured decay length are contradicted by the results reported here.

It is interesting to note that the Fermi velocities inferred from our procedure are different from those derived experimentally[34] from the Fermi surface and cyclotron resonance data since our analysis neglects any velocity enhancements due to electron-phonon coupling effects.

In all three metals, as determined previously,[7–17] the surface state dispersion relations below the Fermi energy lie entirely within the projected band gaps, implying that these are true surface states at these energies. In addition, the ratios of effective masses for the surface state dispersion relations to those of the edges of the respective bulk continua are remarkably constant, as shown in the fourth row of the table. A similar correspondence has been observed previously between *sp* states on Cu(111) and Cu(011).[37] The slight discrepancy between the value shown in Table I for Cu(111) and that quoted in Ref. 34 is due to the more precise estimate of the mass of the edge of the bulk continuum used here. The mechanisms which give rise to these states are all rather similar, and their existence and properties can be predicted within the framework of simple phase analysis models.[38,39] The similarity of these ratios further indicates the similarities among these states, and lends credence to the idea that the surface state effective mass parallel to the surface is largely determined by that of a near by bulk continuum.

### C. Surface-state intensity oscillations

The intensity oscillations observed in Figs. 1 and 2 for both the low- and high-lying states are similar to those observed in a wide variety of simple systems.[16–18,25,40] These have been analyzed to yield simple information concerning the bulk penetration length and oscillation frequency of the surface state's wave function. It will be shown in Sec. IV that these measurements are interesting both from the point of view of surface electronic structure as well as of the behavior of generalized defect states located in band gaps.

The integrated intensities of the high-lying surface states on the three surfaces normalized to the total respective valence-band intensities are plotted in Fig. 7 as a function of final-state momentum normal to the surface, $k_f$, in units of the relevant $L$-point zone boundary momentum. The value of $k_f$ in Å$^{-1}$ is derived from a parametrized free-electron final state:

$$k_f = 0.512[(E_K - V_0)m_f]^{1/2} , \quad (1)$$

where $E_K$ and $V_0$ are the kinetic energy and the inner potential in eV, respectively, and $m_f$ is the final-state effective mass relative to the free electron mass. Over the relatively narrow momentum range shown in Fig. 7, the choice of the two parameters, $m_f$ and $V_0$, is not unique. Without significant loss of accuracy, we fix $V_0$

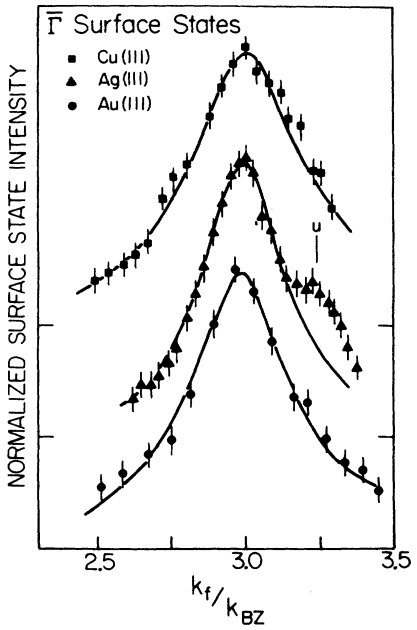


FIG. 7. Intensity of the *sp* surface states on the copper, silver, and gold surfaces as a function of final-state momentum normal to the surface. As explained in the text, these data must maximize near an $L$ point of the bulk band structure. The point labeled $U$ in the silver data indicates the contribution to the surface-state intensity arising from an umklapp process. Solid curves are a fit to the model explained in the text.

to be the energy of the bottom of the bulk band structure, and $m_f$ was adjusted to make our results maximize at $L$, as they must on general grounds (see Sec. IV).[41] The curves in Fig. 7 will be discussed in Sec. IV B.

The derived values of $m_f$ were 1.00, 1.12, and 1.14 for Cu, Ag, and Au, respectively, relative to the free electron mass $m_e$. The final-state dispersion relation is progressively heavier in this sequence. Using a value of $m_f = m_e$ for Ag or Au either shifts the maximum away from $L$ or requires an inner potential of $V_0 \sim -20$ eV, both of which are unphysical. Moreover, a previous investigation of *d*-like surface states on Cu(001) and Ag(001) yielded final masses which were within experimental error of those reported here.[42] Apparently, this heavier final mass is a general phenomenon in silver and gold.

The energies of the final-state bands in gold have been the subject of some controversy in the past. The heavier mass we observe is in approximate accord with bulk band calculations, for which the unoccupied bands can be fitted with an effective mass 10–15% heavier than the free electron bands.[43–45] In addition, a heavy parametrized final state has been used with some success in earlier ARP studies to evaluate the bulk dispersion relations along $\Gamma \rightarrow L$ for silver, gold, and platinum at lower photon energy.[46,47] Other ARP experiments found the unoccupied bands significantly higher than the calculation showed.[48,49] The most recent and probably most accurate ARP study,[50] however, found that the calculated bands at energies 20 eV above the Fermi level were within 0.7 eV of the experimental result. This is in general agreement with our findings here and, by implication, on those on the *d*-like surface state on Ag(001).[42] The conclusion to be drawn from these observations is that the surface states and the bulk states utilize the same final state in exiting the crystal, and that this state has a dispersion relation which can be parametrized by an effective mass 10–15% heavier than the free electron mass.

The reasons for these apparently heavier final states may be related to the distinct *f*-like resonances observed at 20–25 eV above the Fermi level in silver and gold near the center of the bulk Brillouin zone.[43–45] Relativistic effects will tend to pull this higher angular momentum level down in energy, which might result in a higher observed effective mass in the final state. Since this resonance is not present in the copper band structure, one would expect a final-state effective mass in copper distinct from that observed in silver and gold and nearly equal to the observed value of the free electron mass. Further theoretical work will be required to clarify this point.

## IV. DISCUSSION

### A. Au(111) two-dimensional Fermi surface

From the values of $m_s$ and $E_0$ in Table I, the Fermi wave vectors $k_F$ for these parabolic surface state dispersion relations can be determined very precisely. These are shown in the fifth row of the table. Most of the uncertainty in $k_F$ comes from accurately placing the Fermi level in Fig. 3 relative to $E_0$. For Au(111) the value of $k_F$ was measured in a series of azimuths between the $\bar{\Gamma} \rightarrow \bar{M}$ and $\bar{\Gamma} \rightarrow \bar{K}$ lines of the surface Brillouin zone, and was found to be azimuthally isotropic to within $\pm 0.002$ Å$^{-1}$. This is consistent with the isotropy observed in the neck radius for the bulk Fermi surfaces of these metals.[34] Since this *sp* state on all three surfaces is the only intrinsic surface state crossing the Fermi level, the two-dimensional Fermi surface is simply a circle of radius $k_F$.

The large scale reconstruction on this surface has recently been indexed with unit cell dimensions of $23 \times \sqrt{3}$.[28] The value of $k_F$ and the azimuthal isotropy of the Fermi surface imply that this state is not involved in driving the reconstruction, and that some mechanism other than a Fermi surface instability must be operative.

### B. Bulk penetration and complex dispersion relation

The treatment of the surface state intensity oscillations began with the pioneering work of Louie *et al.*,[16] and concerned the very same zone-center state on Cu(111) considered here. That treatment was based on a simple tight-binding analysis. Later work on Al(111) was based on a nearly-free-electron (NFE) model.[24] For the high-lying *sp* surface states considered here, the NFE expansion is more appropriate since these states exist in gaps opened by zone-boundary hybridization and are thus described to a fairly good approximation as Shockley states.[51,52] In addition, a simple phase analysis mod-

el based on the NFE formalism predicts the existence and energies of these states fairly well.[38,39] The analysis and model used to treat the data from Au(111) and Ag(111) in Fig. 7 was used previously to treat data from Cu(111) and is based on an extension of the NFE model using effective mass theory.[25,39] The recent similar work on Ag(111) (Ref. 18) utilized a similar yet somewhat more general and model-independent treatment of the oscillations. Fundamentally, the approximations made were similar to those made here, and the derived values of decay lengths are independent of model, to within the experimental uncertainty.

### 1. *Qualitative observations*

It is useful at this point to consider the general behavior of electronic surface states existing in a projected band gap. The component of momentum of such a state parallel to the surface, $\mathbf{k}_{\parallel}$, is a good quantum number, while the component normal to the surface is complex: $\mathbf{k}_{\perp}=\mathbf{p}+i\mathbf{q}$. The real part, $\mathbf{p}$, is given by the momentum of the nearest bulk band on quite general grounds. In the present case $\mathbf{p}$ is simply $\mathbf{k}_L$, the $L$-point momentum of the bulk band structure. The various lobes of the oscillatory decaying surface state wave function emit in phase with one another when the final-state momentum normal to the surface differs from $\mathbf{k}_L$ by a bulk reciprocal lattice vector. Thus the ARP intensity maximizes at an $L$ point in the extended zone scheme, as observed in Fig. 7. In this sense our measurements are most directly sensitive to $p$, and indirectly to $m_f$. As mentioned previously, there must be some fundamental mechanism which produces an anomalously large value of the parameter $m_f$.

The imaginary part of $\mathbf{k}_{\perp}$, $\mathbf{q}$, is just the inverse of the bulk evanescent decay length for the surface state wave function. If this length is very long, then the frequency spectrum of the state is narrow and the state is observed over a correspondingly narrow range of final-state momenta.[24] Thus the widths of the intensity distributions shown in Fig. 7 are inversely related to the decay length of the state.[25] Qualitatively, the less the splitting of the state from the bulk continuum, $\varepsilon_s$, the less strongly the state is damped and the longer is its decay length. As the splitting vanishes, the surface state becomes indistinguishable from the bulk state at the band edge, and the bulk is penetrated with infinite decay length. The splitting for silver shown in the sixth row of Table I is significantly less than that of copper and gold, and the observed intensity distribution is significantly narrower.

These simple ideas are the basis of a complex band structure, $\varepsilon_s(\mathbf{q})$, which is a measure of the inverse decay length relative to the energy splitting of a surface or defect state from the bulk continuum. As explained above, the point $\mathbf{q}=\mathbf{0}$ on this dispersion relation occurs at $\varepsilon_s=0$. In addition, the curve must be symmetric about $\mathbf{q}=\mathbf{0}$ in systems with a center of inversion, so that the leading term of the complex dispersion relation at small $q$ is quite generally given by

$$\varepsilon_s(\mathbf{q})=3.81q^2/m^* , \tag{2}$$

with $\varepsilon_s$ in eV and $q$ in $\text{Å}^{-1}$, and where $m^*$ is an effective mass. Using effective-mass theory, it is straightforward to predict that $m^*$ will be asymtotically equal in magnitude but opposite in sign to the effective mass of the bulk band nearest in energy to the surface state, taken normal to the surface.[39] In the noble metals, the bulk band structure forms a saddle point at $L$, with the effective mass parallel to the surface nearly isotropic and positive, and with that perpendicular to the surface negative. In what follows, $m^*$ is taken as a free parameter to be derived from the experimental data in Fig. 7 and compared to this simple prediction from effective-mass theory using the effective masses normal to the surface taken from first principles band calculations. The previous paper Cu(111) derived an effective mass which was anomalously large by a factor of more than 2.[25] Our purpose here is to determine whether this effect persists on Ag(111) and Au(111).

### 2. *Model for surface-state intensity*

The NFE model for surface state intensity oscillations, elaborated in its simplest form previously for Al(111),[24] is applicable to the present case as well. However, the much larger lattice potentials and band gaps involved in the noble metals relative to aluminum suggest some improvements. As first suggested by Louie,[16] the surface state wave function $\Psi_S$ is expanded in terms of those of the bulk bands $\Psi_B$ of band index $n$:

$$\Psi_S=\sum_{n,\mathbf{k}}\alpha(n,\mathbf{k})\Psi_B(n,\mathbf{k}) . \tag{3}$$

Since $\mathbf{k}_{\parallel}$ is a good quantum number for the surface state, those bulk states at the appropriate $\mathbf{k}_{\parallel}$ (zero in this zone center case) are projected in the sum, leaving the sum over $\mathbf{k}_{\perp}$ and $n$ only. The surface state intensity $I_S$ at an energy corresponding to the final state $\langle \mathbf{k}_f \mid$ is given by Fermi's golden rule:

$$\begin{aligned} I_S &\sim |\langle \mathbf{k}_f \mid \mathbf{A}\cdot\mathbf{p} \mid \Psi_S \rangle|^2 \\ &\sim \left| \sum_{n,\mathbf{k}} \langle \mathbf{k}_f \mid \mathbf{A}\cdot\mathbf{p} \mid \Psi_B(n,\mathbf{k}_{\perp})\rangle \alpha(n,\mathbf{k}_{\perp}) \right|^2 \\ &\sim \left| \sum_{n,\mathbf{k}} M_B(n,\mathbf{k}_{\perp})\alpha(n,\mathbf{k}_{\perp})\delta(\mathbf{k}_f-\mathbf{k}_{\perp}-\mathbf{G}) \right|^2 \\ &\sim \left| \sum_{n,\mathbf{G}} M_B(n,\mathbf{k}_f-\mathbf{G})\alpha(n,\mathbf{k}_f-\mathbf{G}) \right|^2 . \end{aligned} \tag{4}$$

The final two steps rely on direct momentum conserving transitions between bulk bands governed by momentum matrix elements $M_B(n,\mathbf{k}_f-\mathbf{G})$.[53,54] This is an approximation which will be considered shortly. These results are analogous to the geometric structure factor and the unit cell form factors introduced by Hsieh *et al.*[18] Normally, the primary Mahan cone[55] dominates and only one reciprocal lattice vector $\mathbf{G}$ contributes. In the analysis for Ag(111) below, we have found an exception to this expectation.

In the spirit of the effective-mass-theory-modified NFE approximation, $|\Psi_B\rangle$, $|\Psi_S\rangle$, and $|\mathbf{k}_f\rangle$ are all taken to have the NFE wave-function form. For bulk states,

$$\Psi_B(n,\mathbf{k})=\sum_{\mathbf{G}} c_n(\mathbf{k},\mathbf{G})e^{i\mathbf{k}\cdot\mathbf{G}} . \quad (5)$$

In principle, this sum runs over all three-dimensional reciprocal lattice vectors. In the present case, however, the symmetry of normal emission eliminates all but the two vectors $\mathbf{G}=(000)$ and $\mathbf{G}=(\overline{111})2\pi/a$. Without losing any accuracy, the sum reduces to one dimension and two terms:

$$\Psi_B(n,\mathbf{k})=c_0(k)e^{ikz}+c_1(k)e^{i(k+g)z} , \quad (6)$$

where $g=\sqrt{3}(2\pi/a)$ and $a$ is the bulk lattice constant. The coefficients $c_n(k)$ can be easily evaluated. In principle, $\langle \mathbf{k}_f |$ can be derived in the same fashion, but in practice, near the maximum in intensity, one term is normally sufficient. $|\Psi_S\rangle$ is taken to have the NFE form

$$\Psi_S \cong \begin{cases} e^{qz}\cos(k_L z+\delta), & z<z_0 \\ e^{-pz}, & z>z_0, \end{cases}$$

where the parameters $q$, $\delta$, and $p$ are taken from effective-mass theory.[39] The small $q$ form for the complex dispersion relation in Eq. (2) is sufficient for these states which lie close to the bottom of the band gap. The simple exponential decay outside the surface is not correct since the surface barrier potential is not rectangular. The contribution of this part of the wave function to the photoemission intensity, however, is small, and the approximate form is quite adequate.

As explained previously, in the fit performed below, we first choose the final-state effective mass $m_f$ in order to force the maximum intensity to occur at an $L$ point in the extended zone scheme. The next most sensitive parameter is $q$, the inverse decay length, since this determines the width of the intensity distribution. In the iteration procedure the effective mass of the complex dispersion relation $m^*$ is taken to be a free parameter, with the value of $q$ being calculated from Eq. (2) using the values of $\varepsilon_s$ derived from the procedure explained earlier.

Using these wave functions, the parameters $\alpha(n,\mathbf{k}_f-\mathbf{G})$ and $M_B$ can be calculated analytically, leading to an analytic expression for $I_S(\mathbf{k}_\perp)$. The resulting value of $m^*$ is not expected to be very sensitive to these parameters since we fit primarily the width of the intensity distribution and these parameters are smooth functions of $\mathbf{k}_\perp$ regardless of how they are evaluated. This assumption of smoothness neglects any effects from final-state scattering (photoelectron diffraction), which is a good approximation for these delocalized initial states.

A further refinement of the model is to introduce some damping into the final state, as was done in treating Al(111) and Cu(111).[17,24,25] Hsieh *et al.*[18] included this effect in their more general treatment as well. This damping is equivalent to relaxing the $\delta$ function in the direct transition matrix elements [Eq. (4)] by Lorentzian lifetime broadening.[53,54,56] The broadening corresponds to the inverse of the final-state elastic mean free path, quantities which have been measured for the noble metals in this energy range.[56,57] We have fixed this length at 5 Å for all three metals. The uncertainty of this parameter of $\pm 1$ Å endows our estimate of the surface state decay length with nearly the same uncertainty, and in addition acts to justify some of the simplifications introduced above.

### 3. Derivation of $m^*$

The curves in Fig. 7 represent the best fits of this model to our experimental data. The results for copper have appeared earlier[25] and yielded an anomalously high value of $m^*$ shown in the seventh row of Table I. The experimental results for Ag(111) show a distinct shoulder near $h\nu=60$ eV. This corresponds very closely to the energy expected for sampling an $L$ point of the bulk bands via an umklapp process using the bulk reciprocal lattice vector $\mathbf{G}=(2,2,0)2\pi/a$ rather than $\mathbf{G}=(1,1,1)2\pi/a$.[56] There is also apparent some broadening on the high momentum sides of the Au(111) and the Cu(111) intensity distributions, presumably for the same reason. The shorter surface state decay lengths for the copper and gold surfaces lead to inherently broader distributions so that these umklapp features are less apparent. Their effect on the parameters derived from the fit are negligible in copper and gold. For Ag(111), the data set was truncated prior to fitting at $h\nu=51$ eV, in order to avoid the effect of this shoulder. Note that over the energy ranges plotted, this $(2\bar{2}0)$ umklapp is the only one that could interfere in this way, lending general credence to our single-beam final state. The integrated intensity in these umklapp features is $\sim 10\%$ of that arising from the normal process, in accord with previous experimental results.[56] The necessity of truncating our data set for Ag(111), coupled to the larger relative contribution from final-state damping to the width of the intensity distribution, clearly renders our results for this surface less accurate.

The previous study of the Ag(111) state by Hsieh *et al.*[18] utilized a final-state effective mass equal to the free electron mass in Eq. (1), so that the shoulder coincidentally occurs at an $L$ point for the normal process with $\mathbf{G}=(1,1,1)2\pi/a$. The larger peak is thus shifted to a lower momentum and a good explanation for its occurance was lacking. Our analysis utilizing a heavier final-state mass gives more consistent results for these (111) surface states as well as for the Ag(001) $d$-like surface state.[42] Further theoretical work concerning the final-state dispersion relations is advisable.

Values of $|m^*|/m_e$ for band 6 at $\mathbf{k}_L$ evaluated normal to the surface derived from bulk band calculations[43–45] vary within 5–10% of 0.25, 0.14, and 0.16 for copper, silver, and gold, respectively. In each case these are roughly one-half the values derived from our fits in Fig. 7 and shown in the seventh row of the table. Apparently, the anomalies observed in Cu(111) are preserved in the similar states on Ag(111) and Au(111). Locally, in some sense, the bulk band behaves near the defect state as though it were heavier than it does deep in the bulk of the material. For Cu(111), this behavior has been seen directly in the real band structure measured by photoemission.[58,59] In silver and gold the intensity in band 6 is so small and the bulk direct transition peak so broad that we were unable to derive accu-

rate dispersion relations for the real bands near $L$.

The derived values of the $m^*$ and the energy splittings $\varepsilon_s$ yield the decay lengths shown in the final row of the table. As noted before, the result for Cu(111) is in good accord with recent nearly-first-principles local-density-approximation (LDA) calculations.[21–23] Our results for Ag(111) are smaller by a factor of 2 than those reported by in Ref. 14 using a very different experimental procedure wherein the surface-state energy shifts induced by a buried layer of gold were interpreted to yield a decay length. Perhaps the buried layer produced a larger perturbation than expected in that case. The analysis in Ref. 18 relied on the measure decay length determined in Ref. 12 and thus cannot be directly compared to our results.

## V. SUMMARY AND CONCLUSIONS

There are two general conclusions to be drawn from the results summarized in Table I. The first is the generally quite satisfactory level of accord seen between experimental and calculated results. The accord for Cu(111) is nearly the best that has been seen in any system, and that Ag(111) and Au(111) is also quite respectable considering the difficulty of electronic structure calculations on these heavier metals. This observation is at first surprising since the calculations are performed in the density functional formalism and all make the LDA. They should therefore not really be compared to a photoemission experiment which measures an excitation spectrum. The observed accord is probably due to the fact that these initial states are located energetically very close to the Fermi level. In the sense of Fermi-liquid theory, the final-state photohole is not highly excited. Thus the quasiparticle lifetime is quite long, as evidenced by our narrow observed linewidths, and one might hope to observe good accord with a ground-state calculation.

The second important conclusion concerns the consistent disagreement between our measured values of $m^*$ and those expected by applying effective-mass theory and using calculated bulk effective masses near $L$. One possible reason for this anomaly is the use of the LDA in the bulk calculations. Using this calculational approach in the vicinity of an absolute band gap has been wrought with difficulty in the past: the calculated band gaps of tetrahedral semiconductors are predicted to be 30–50% smaller than experimental values.[60,61] This anomaly might present itself in these noble-metal projected gaps as well, a prediction supported by the general difficulty that first-principles calculations have had in producing the right width of the gap at $L$ in the noble metals.[35] One might also expect that these would produce errant values for the effective masses near the band gap.

The two most recent calculations of the Cu(111) surface, however, have both been performed using the LDA, and both can be used to predict penetration lengths in rather good accord with our results.[22,23] These projected gaps do not present as serious a singularity as an absolute gap in a semiconductor. While the weaknesses of the LDA methods cannot be excluded from our consideration, an investigation of other possible sources for the anomaly are in order.

An explanation proposed previously involved perturbations on the bulk band contours near a defect state.[25,58,59] This can be viewed in the following way. The surface-state wave function must be orthogonal to all bulk wave functions. This is particularly difficult to arrange for bulk states in the vicinity of the $L$ point due to the fact that the frequency spectrum of the surface-state wave function is centered there. One way for the orthogonalization to be accomplished is for the surface state to be repelled from the bulk and for the bulk state to be repelled from the vicinity of the surface. There is direct experimental evidence for this phenomenon in Figs. 1 and 2, where the bulk band vanishes as the surface-state intensity maximizes. The bulk wave function apparently decays before it approaches the surface to within the sampling depth of the photoemission probe. Moreover, a surface slab calculation includes this orthogonalization effect automatically, and would thus be expected to produce the good estimates of the penetration length. A calculation of the bulk band structure, however, does not include any defect states. To append a surface state to a bulk calculation in the spirit of nearly-free-electron or effective-mass theory really produces an overcomplete basis set, and direct comparison of observed defect properties with calculated bulk properties is not entirely valid. Our results should be differentiated in this respect from tunneling studies[62,63] in semiconductors where no intrinsic defect state need be involved, and experimental results can be predicted with greater accuracy from bulk band calculations.

## ACKNOWLEDGMENTS

We wish to acknowledge N. G. Stoffel for his help in the early work on these experiments, and N. V. Smith and R. Haydock for numerous helpful discussions. This work was carried out in part at the National Synchrotron Light Source NSLS, Brookhaven National Laboratory, which is supported by the U.S. Department of Energy (Division of Materials Sciences and Division of Chemical Sciences). Financial support from the U.S. Department of Energy under Grant No. DE-FG06-86ER45275 and from the American Chemical Society Petroleum Research Fund is gratefully acknowledged.

[1] E. W. Plummer and W. Eberhardt, *Advances in Chemical Physics* (Wiley, New York, 1982), Vol. 49.

[2] F. Forstmann, in *Photoemission and the Electronic Properties of Surfaces,* edited by B. Feuerbacher, B. Fitton, and R. F. Willis (Wiley, New York, 1978).

[3] S. D. Kevan, Phys. Rev. B **28**, 2268 (1983).

[4] A. Euceda, D. M. Bylander, L. Kleinman, and K. Mednick, Phys. Rev. B **27**, 659 (1983).

[5] S. D. Kevan, Phys. Rev. B **33**, 4364 (1986).

[6] S. D. Kevan, Surf. Sci. **178**, 229 (1986).

[7]P. O. Gartland and B. J. Slagsvold, Phys. Rev. B **12**, 4047 (1975).
[8]P. Heimann, H. Neddermeyer, and H. F. Roloff, J. Phys. C **10**, L17 (1977).
[9]P. Heimann, J. Hermann, H. Miosga, and H. Neddermeyer, Surf. Sci. **85**, 263 (1979).
[10]R. Courths, H. Wern, U. Hau, B. Cord, V. Bachelier, and S. Hufner, J. Phys. F **14**, 1559 (1984).
[11]S. D. Kevan, Phys. Rev. Lett. **50**, 526 (1983).
[12]G. V. Hansson and B. J. Slagsvold, Phys. Rev. B **17**, 473 (1978).
[13]G. V. Hansson and S. A. Flodstrom, Phys. Rev. B **18**, 1572 (1978).
[14]T. C. Hsieh, T. Miller, and T.-C. Chiang, Phys. Rev. Lett. **55**, 2483 (1985).
[15]Z. Hussain and N. V. Smith, Phys. Lett. **66A**, 492 (1978).
[16]S. G. Louie, P. Thiry, R. Pinchaux, Y. Petroff, D. Chandesris, and J. Lecante, Phys. Rev. Lett. **44**, 549 (1980).
[17]S. D. Kevan, N. G. Stoffel, and N. V. Smith, Phys. Rev. B **31**, 3348 (1985).
[18]T. C. Hsieh, P. John, T. Miller, and T.-C. Chaing, Phys. Rev. B **35**, 3728 (1987).
[19]K. M. Ho, C. L. Fu, S. H. Liu, D. M. Kolb, G. Piazza, J. Electroanal. Chem. **150**, 235 (1983).
[20]S. H. Liu, C. Hinnen, C. Nguyen van Huong, and N. R. De Tacconi, K. M. Ho, J. Electroanal. Chem. **176**, 325 (1984).
[21]A. Euceda, D. M. Bylander, and L. Kleinman, Phys. Rev. B **28**, 528 (1983).
[22]J. A. Appelbaum and D. R. Hamann, Solid State Commun. **27**, 881 (1978).
[23]J. A. Verges and E. Louis, Solid State Commun. **22**, 663 (1977).
[24]S. D. Kevan, N. G. Stoffel, and N. V. Smith, Phys. Rev. B **31**, 1788 (1985).
[25]S. D. Kevan and R. H. Gaylord, Phys. Rev. Lett. **57**, 2795 (1986).
[26]M. A. Van Hove, R. J. Koestner, P. C. Stair, J. P. Biberian, L. L. Kesmodel, I. Bartos, and G. A. Somorjai, Surf. Sci. **102**, 189 (1983).
[27]J. Perdereau, J. P. Biberian, and G. E. Rhead, J. Phys. F **4**, 798 (1974).
[28]U. Harten, A. M. Lakee, J. P. Toennies, and Ch. Woll, Phys. Rev. Lett. **54**, 2619 (1985).
[29]W. J. M. Tegart, *Electrolytic and Chemical Polishing of Metals* (Pergamon, New York, 1959).
[30]P. Thiry, P. A. Bennett, S. D. Kevan, W. A. Royer, E. E. Chaban, J. E. Rowe, and N. V. Smith, Nucl. Instrum. Methods **222**, 85 (1984).
[31]S. D. Kevan, Rev. Sci. Instrum. **54**, 1441 (1983).
[32]B. Reihl, K. H. Frank, and A. Otto, Z. Phys. B **62**, 473 (1986).
[33]J. Kanski, P. O. Nilsson, and C. G. Larsson, Solid State Commun. **35**, 397 (1980).
[34]M. R. Halse, Philos, Trans. R. Soc., Ser. A **265**, 507 (1969).
[35]D. P. Woodruff, W. A. Royer, and N. V. Smith, Phys. Rev. B **34**, 764 (1986).
[36]N. V. Smith, Phys. Rev. B **24**, 1895 (1981).
[37]S. D. Kevan, Phys. Rev. B **28**, 4822 (1983).
[38]N. V. Smith, Phys. Rev. B **32**, 3549 (1985).
[39]S. D. Kevan, Phys. Rev. B **34**, 6713 (1986).
[40]H. J. Levinson, F. Greuter, and E. W. Plummer, Phys. Rev. B **27**, 727 (1983).
[41]N. W. Ashcroft and N. D. Mermin, *Solid State Physics* (Holt, Rinehardt, and Winston, New York, 1976).
[42]S. D. Kevan and N. G. Stoffel, Phys. Rev. B **32**, 4956 (1985).
[43]N. E. Christensen, Phys. Status Solidi B **54**, 551 (1972).
[44]N. E. Christensen and B. O. Seraphin, Phys. Rev. B **4**, 3321 (1979).
[45]H. Eckardt, L. Fritsche, and H. Noffke, J. Phys. F **14**, 97 (1984).
[46]P. S. Wehner, R. S. Williams, S. D. Kevan, D. Denley, and D. A. Shirley, Phys. Rev. B **19**, 6164 (1979).
[47]K. A. Mills, R. F. Davis, S. D. Kevan, G. Thornton, and D. A. Shirley, Phys. Rev. B **22**, 581 (1980).
[48]P. Heimann, H. Miosga, and H. Neddermeyer, Solid State Commun. **29**, 463 (1979).
[49]R. Rosei, R. Lasser, N. V. Smith, and R. L. Benbow, Solid State Commun. **35**, 979 (1980).
[50]R. Courths, H.-G. Zimmer, A. Goldmann, and H. Saalfeld, Phys. Rev. B **34**, 3577 (1986).
[51]W. Shockley, Phys. Rev. **56**, 317 (1939).
[52]E. T. Goodwin, Proc. Cambridge Philos. Soc. **35**, 221 (1939).
[53]J. A. Knapp, F. J. Himpsel, and D. E. Eastman, Phys. Rev. B **19**, 4952 (1979).
[54]P. Thiry, D. Chandesris, J. Lecante, C. Guillot, R. Pinchaux, and Y. Petroff, Phys. Rev. Lett. **43**, 82 (1979).
[55]G. D. Mahan, Phys. Rev. B **2**, 4334 (1971).
[56]F. J. Himpsel and W. Eberhardt, Solid State Commun. **31**, 747 (1979).
[57]H. Ibach, *Electron Spectroscopy for Surface Analysis* (Springer, Berlin, 1978), p. 5.
[58]P. Thiry, PhD. thesis, Université de Paris–Sud (1980).
[59]P. Thiry and Y. Petroff, Appl. Opt. **19**, 3957 (1980).
[60]M. S. Hybertson and S. G. Louie, Phys. Rev. Lett. **55**, 1418 (1985).
[61]C. S. Wang and W. E. Pickett, Phys. Rev. Lett. **51**, 597 (1983).
[62]G. H. Parker and C. A. Mead, Phys. Rev. Lett. **21**, 605 (1968).
[63]S. Kurtin, T. C. McGill, and C. A. Mead, Phys. Rev. Lett. **25**, 756 (1970).